



Kinetic and mechanism studies of musk tonalide reacted with hydroxyl radical and the risk assessment of degradation products

Hansun Fang^{a,c}, Guiying Li^b, Side Yao^d, Ximei Liang^e, Taicheng An^{b,c,*}

^a School of Environmental and Land Resource Management, Jiangxi Agricultural University, 1101 Zhimin Road, Nanchang 330045, China

^b Institute of Environmental Health and Pollution Control, School of Environmental Science and Engineering, Guangdong University of Technology, Guangzhou 510006, China

^c State Key Laboratory of Organic Geochemistry and Guangdong Key Laboratory of Environmental Resources Utilization and Protection, Guangzhou Institute of Geochemistry, Chinese Academy of Sciences, Guangzhou 510640, China

^d Shanghai Institute of Applied Physics, Chinese Academy of Sciences, Shanghai 201800, China

^e School of Animal Science and Technology, Jiangxi Agricultural University, 1101 Zhimin Road, Nanchang 330045, China

ARTICLE INFO

Article history:

Received 29 January 2016

Received in revised form 28 March 2016

Accepted 10 June 2016

Available online 24 June 2016

Keywords:

Tonalide

Hydroxyl radical

Laser flash photolysis

Risk assessment

ABSTRACT

Tonalide was extensively used as fragrances in various personal care products and recognized as emerging contaminant recently. In this study, the transient reactions of hydrophobic tonalide with hydroxyl radical ($\cdot\text{OH}$), one of highly reactive oxygen species (ROs), was firstly investigated in acetonitrile through direct observation using laser flash photolysis. Two transient intermediates were formed with the peak centered at 360 and 450 nm, and the bimolecular reaction rate constants of tonalide with $\cdot\text{OH}$ were determined in both water and acetonitrile solutions with values of 4.04×10^9 and $1.95 \times 10^9 \text{ M}^{-1} \text{ s}^{-1}$, respectively. Then, the photocatalytic experiments in a heterogeneous TiO_2 system were carried out to study the decomposition kinetics of tonalide with $\cdot\text{OH}$, which was confirmed as the dominant ROs in photocatalytic system. Five degradation products were identified with molecule weight of 260, 272 and 274. Finally, the potential risks of reaction products formed through the reactions of tonalide with $\cdot\text{OH}$ were further investigated. It is found that the toxicity towards luminescent bacterium (*Photobacterium phosphoreum*) was not changed so much, and the estrogenic activity increased a little bit during the degradation of tonalide by $\cdot\text{OH}$.

© 2016 Elsevier B.V. All rights reserved.

1. Introduction

Polycyclic musk compounds belong to synthetic musk which were typical ingredient of cosmetic and household commodities, such as perfumes, body lotion, soaps, deodorants, and detergents [1,2]. Although the musk in products was usually below 2% [3], the consumption of fragrant products was very huge all over the world, and the discharging of polycyclic musk through wastewater could raise persistent pollution problems in natural waters. Plenty reports found that polycyclic musk distributed widely in various natural aqueous environment, like sea waters [4], fresh waters [5], sediments [6], as well as the body of aquatic organisms around the world [7]. Moreover, polycyclic musk would not only contaminate the aqueous environment, but also tend to accumulate in the

hydrophobic and non-aqueous phases in nature system, due to the high octanol-water partition coefficients for most species of them [8]. As such, some researchers even suggested using synthetic musk as the anthropogenic markers of domestic wastewater [9].

Furthermore, some negative effects were observed by accumulated polycyclic musk in organisms. For example, in the aspect of plants, polycyclic musk was found to inhibit the seed germination and seedling growth of wheat [10]. As to aqueous organisms, polycyclic musk would affect the heart rate of zebrafish larvae [11], and suppress the juvenile development and arise mortality rate of copepod [12]. At molecular level, the toxic mechanism of polycyclic musk were found to cause estrogenic effects [13], genetic injuries [14], gene expression disturbing [15], as well as the cellular xenobiotic defense system damaging [16]. Therefore, both the persistent existence and potential environmental concerns required the investigations on decomposition characteristics, fate and potential risk of polycyclic musk in nature environment.

In natural aqueous systems, photolysis, especially the indirect photodegradation plays an important role in the decomposition of organic pollutants [17]. Hence, to precisely and comprehensively

* Corresponding author at: Institute of Environmental Health and Pollution Control, School of Environmental Science and Engineering, Guangdong University of Technology, Guangzhou 510006, China.

E-mail address: antc99@gdut.edu.cn (T. An).

understand and predict the fate of polycyclic musk compounds in nature, the degradation of polycyclic musk during indirect photolysis should also be clearly clarified. The indirect photolysis in nature aqueous environment was mainly initiated by reactive oxygen species (ROSs) [18]. Among the ROSs, hydroxyl radical ($\bullet\text{OH}$) with oxidation-reduction potential up to 2.8 V is considered the most reactive specie, which is able to rapidly decompose the alkane and aromatic organic compounds with constants near molecular diffusion rates [19]. As a typical group of emerging organic pollutants, polycyclic musk was composed of aliphatic structures and a benzene ring, thereby implying that they could also be efficiently degraded by $\bullet\text{OH}$. Though the photochemical degradation of polycyclic musk has been studied in several reports, the engagement of ROSs like $\bullet\text{OH}$ in the reaction was either ignored, or just mentioned without direct evidence [20]. For example, the transient reaction spectra and the precise values of bimolecular reaction rate constants (k) of $\bullet\text{OH}$ reacting with musk were barely discussed [21,22]. Moreover, the studies on the $\bullet\text{OH}$ -based advanced oxidation of polycyclic musk were all performed in aqueous rather than non-aqueous solution [23,24]. As such, it could be largely ignored some important transformation process of polycyclic musk compounds with $\bullet\text{OH}$, since polycyclic musk compounds were tend to accumulate in lipid or organic rich samples in natural aqueous systems, such as sludge, sediments or even fatty tissue of aquatic organisms [7,25]. To model the physicochemical reactions in or on the surface of natural non-aqueous environment, pure organic solvent or compounds with weak polarity and hydrogen bond were always adopted, such as acetonitrile, tetrahydrofuran, wax films and heptane [26–29], and these methods made it more meaningful and appropriately to study the kinetics of $\bullet\text{OH}$ with polycyclic musk in non-aqueous or hydrophobic environmental conditions, where the studies were still limited. Last but not least, though the negative effects of parental compounds have been studied, the potential risks of transformation products resulted from the reactions of polycyclic musk with naturally occurred ROSs such as $\bullet\text{OH}$ have not been well clarified yet.

Hence, an extensively used commercial polycyclic musk compound, tonalide was selected as the typical example of polycyclic musk to study its reactions with $\bullet\text{OH}$. Considering acetonitrile was ideal solvent with the weak polarity, high dissolving capacity towards tonalide and relatively low bimolecular rate constant with $\bullet\text{OH}$ ($3.7 \times 10^7 \text{ M}^{-1} \text{ s}^{-1}$) [19], we decided to adopt this commonly used organic solution to study the non-aqueous reactions of $\bullet\text{OH}$ with tonalide. Firstly, the transient spectra of $\bullet\text{OH}$ reacting with tonalide was studied in detail in a pure acetonitrile solution, where $\bullet\text{OH}$ was yield by laser flash photolysis of N-hydroxypyridine-2-thione (PSH). Secondly, to fully understand the degradation kinetics of tonalide both in water and non-aqueous environment such as the interior of sediment organic matter, the values of bimolecular rate constant (k) were measured and compared both in aqueous and non-aqueous acetonitrile solutions. Then, the photocatalytic TiO_2 system was used as a model system of $\bullet\text{OH}$ -based degradation, further illustrated the role of $\bullet\text{OH}$ in the tonalide degradation kinetics by several scavenging experiments, and the main degradation products were also determined. Finally, the mixtures of tonalide degradation products were extracted, and the evolution of ecotoxicity and estrogenic activity of tonalide during the degradation by $\bullet\text{OH}$ were evaluated.

2. Experimental section

2.1. Materials

Tonalide (purity $\geq 95\%$) and hexamethylbenzene (HMB, purity $\geq 97\%$) were purchased from Adamas Reagent Ltd, Shanghai,

China. N-hydroxypyridine-2-thione (PSH), *trans*-stilbene (TS) and methyl methacrylate (MMA) were obtained from J&K Chemical Ltd (purity $\geq 99\%$). TiO_2 nanoparticles (Degussa P25, 80% anatase, 20% rutile), nano aluminum oxide (Al_2O_3), HPLC grade acetonitrile, high-purity nitrogen (N_2) as well as other reagents were used as received. Luminescent bacterium (*Photobacterium phosphoreum*) was obtained from the Institute of Soil Science, Chinese Academy of Sciences, China. Estrogenic activity assay kit was from Research Center for Eco-Environmental Sciences, Chinese Academy of Sciences, China.

2.2. Laser flash photolysis

Laser flash photolysis was carried out using a Nd:YAG laser, and the 355 nm laser pulse with duration of 5 ns was used at the energy of 10–15 mJ per pulse. A xenon lamp was employed as detecting light source, and the laser and analyzing light beam passed perpendicularly through a 1×10 mm slit and then to a $10 \times 10 \times 40$ mm quartz cell for the reaction. The transmitted light entered a monochromator equipped with an R955 photomultiplier. The output signal from the HP54510B digital oscillograph was transferred to a personal computer for further data analysis. All of the measurements were carried out at room temperature (25°C) immediately after the preparation. For laser flash photolysis, all experiments were performed under anaerobic condition achieved by degassing with high-purity N_2 .

2.3. Heterogeneous photocatalysis

Decomposition kinetics of tonalide and characterization of the role of $\bullet\text{OH}$ were performed in constantly-stirred slurry of particular TiO_2 (2.0 g L^{-1}) with 50 μM tonalide: 2 mL tonalide stock solution (1.5 mM in acetonitrile) was firstly added into the reactor with 120 mg TiO_2 . Mix the solution homogeneously for 20 min and then evaporate the acetonitrile by N_2 blowing. Finally, 60 mL water was filled, and the heterogeneous aqueous solution was prepared by mix homogeneously for another 20 min. A 300 W high-pressure mercury lamp system with a 340 nm cutoff filter was used as the light source as described elsewhere [30]. The heterogeneous solution (5 mL) was sampled at specific time and extracted by hexane three times (1.0 mL each time). The hexane extracts were then combined and dehydrate with 0.1 g Na_2SO_4 . The concentration of tonalide was measured on a HP-5 column (60 m \times 0.25 mm id, 0.25 μm thickness) by gas chromatography-mass spectrometer (GC-MS, Agilent 6890, Agilent, CA, USA) with mass to charge ratio (m/z) of 243.2. Injection temperature was 260°C . Temperature of column oven was firstly hold on 80°C for 1 min, then increased from 80 to 280°C with a gradient of $10^\circ\text{C min}^{-1}$, and hold 280°C for 1 min.

To identify the main degradation products, 100 μM tonalide in 2.0 g L^{-1} heterogeneous TiO_2 were prepared, and the photocatalysis reaction was terminated at 30 min. Sixty milliliters of the heterogeneous solution was extracted by hexane for three times (15 mL each time). The extracted solution was combined and dehydrated with Na_2SO_4 , and then evaporated to about 10 mL with a rotary evaporator. Finally, the extract was concentrated and made up to 1.0 mL by nitrogen blow, and 1.0 μL of the extracted sample was directly analyzed by GC-MS. The conditions for GC-MS operation were the same as kinetic studies described above.

2.4. Scavenging experiments

For laser flash photolysis in acetonitrile, 1 M *t*-butanol was used to quench $\bullet\text{OH}$, and methyl methacrylate (MMA, 1 M) was used to quench both $\bullet\text{OH}$ and 2-pyridylthiyl radical (PyS^\bullet) [26]. For the heterogeneous photocatalysis in aqueous TiO_2 , TiO_2 was replaced

by Al₂O₃ (without photocatalytic activity) to determine the direct photochemical degradation of tonalide. Then, 1 M methanol was used to quench •OH and photogenerated holes (h⁺) in aqueous, and acetonitrile was adopted to replace water as the solvent to exclude •OH [31]. The pseudo-first-order rate constants (k₁) for TiO₂ photocatalytic degradation kinetics were all measured with methods and equations showed in Supporting Information.

2.5. Determination of the bimolecular reaction rate constants

Laser flash photolysis was used to determine the bimolecular reaction rate constants in acetonitrile (k_{tonalide,acetonitrile}). Solution (2.0 mL) consisted of PSH (0.3 mM), *trans*-stilbene (TS, held constant at 4.0 mM) and different concentrations of tonalide (serial concentrations between 0 and 90 mM) was prepared. The dependence of maximum transient absorbance intensity at 392 nm (absorption of intermediates formed by TS reaction with •OH) was measured at specific tonalide concentration, and k_{tonalide,acetonitrile} was calculated based on Stern-Volmer equation expressed as Eq. (1):

$$\frac{A_0}{A} = 1 + \frac{k_{\text{tonalide, acetonitrile}}[\text{tonalide}]}{k_{\text{TS, acetonitrile}}[\text{TS}]} \quad (1)$$

where A₀ is the maximum absorbance intensity at 392 nm measured for 0 mM tonalide, A is the absorbance of 392 nm when specific concentration of tonalide is presented, and k_{TS,acetonitrile} refers to the bimolecular reaction rate constant of •OH with TS (6.1 × 10⁹ M⁻¹ s⁻¹) [27].

Fenton reaction system was used to determine the reaction rate constants in water (k_{tonalide,water}). Solution is consisted of 20 μM FeSO₄, 300 μM H₂O₂, 200 μg L⁻¹ tonalide, and 140 μg L⁻¹ HMB. 5 mL samples at different time intervals of 0, 5, 10, 15, 20, 30, 40, 50, 60 s were collected and added 50 μL methanol to scavenge •OH immediately. Tonalide and HMB were extracted by disperse liquid-liquid phase microextraction (DLLME, details were depicted in Supporting Information) [32], and determined by GC-MS. Then, k_{tonalide,water} was obtained as shown in Eq. (2) [33]:

$$\ln \frac{[\text{HMB}]_t}{[\text{HMB}]_0} = \frac{k_{\text{HMB, water}}}{k_{\text{tonalide, water}}} \ln \frac{[\text{tonalide}]_t}{[\text{tonalide}]_0} \quad (2)$$

where k_{HMB,water} refers to the bimolecular reaction rate constant of •OH with HMB (7.2 × 10⁹ M⁻¹ s⁻¹) [19].

2.6. Ecotoxicity and estrogenic activity assessments

The evolution of ecotoxicity and estrogenic activity during the photocatalysis process of 50 μM tonalide with •OH were evaluated by the luminescent of *P. phosphoreum* and the β-galactosidase activity of recombination yeast cells, and the detailed experimental methods and procedures were described in Supporting Information [30].

3. Results and discussion

3.1. Steady-state absorption spectra

The steady-state absorption spectra of PSH and tonalide in acetonitrile are shown in Fig. 1. At the laser flash photolysis excitation wavelength of 355 nm, the absorbance of PSH and tonalide was 1.80 and 0, respectively, suggesting direct photochemical reactions of tonalide should not occurred by direct photolysis, and only PSH would be excited in PSH-tonalide mixtures under the laser flash photolysis experimental conditions.

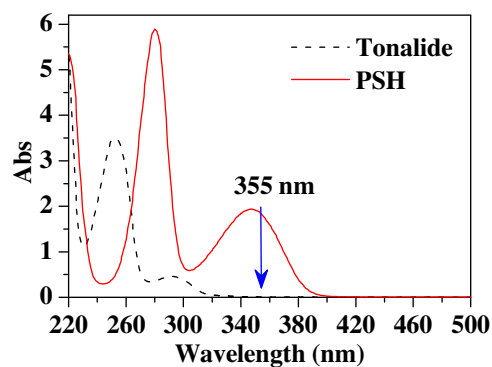


Fig. 1. UV-Vis absorption spectra of 0.4 mM PSH and 0.3 mM tonalide in acetonitrile. Arrow indicates the excitation wavelength of laser flash photolysis (λ_{ex} = 355 nm).

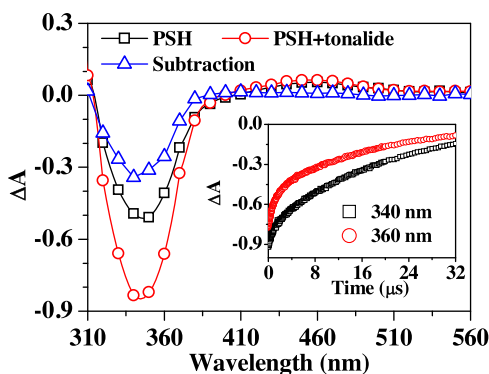


Fig. 2. Subtraction spectra (Δ) and the original transient absorption spectra of 0.3 mM PSH (□) and PSH-tonalide mixtures (0.3 mM PSH with 0.4 mM tonalide, ○) in acetonitrile photo-excited at 355 nm under anaerobic conditions at 0.5 μs. Inset presents the corresponding time evolution profiles probed at 340 and 360 nm of PSH-tonalide mixtures under anaerobic conditions.

3.2. Transient absorption spectra

The UV-Vis transient absorption spectra of PSH and PSH-tonalide mixtures in acetonitrile following 355 nm excitation under anaerobic conditions were recorded at 0.5 μs as shown in Fig. 2. The bleaching in spectra from 310 to 400 nm was ascribed to the direct photolysis of PSH, resulting in the formation of •OH and PyS^{*} [27]. The broad band formed at 400–510 nm would be mainly due to the superposition of PyS^{*}, which was also found to possess relativities toward various organic substrates [34]. To distinguish the transient intermediates formed by tonalide from the products of photo-excited PSH, the spectra of pure PSH was subtracted from the combination spectra obtained in PSH-tonalide mixtures, and the formation of PyS^{*} (400–510 nm) could be eliminated as shown in the subtraction spectra in Fig. 2. These results indicate it might be possible to observe the intermediates formed by tonalide with •OH directly by eliminating the background spectra interference through subtraction method.

To further characterize the new intermediates formed by tonalide, the subtraction spectra at different intervals from 0.5 to 15.0 μs are recorded in Fig. 3. A wide broad increase in the subtraction spectra was observed from 390 to 500 nm (enlarged view is presented in the inset of Fig. 3), which might be attribute to the absorbance of the intermediates formed by tonalide with •OH. However, due to PSH was not a specific •OH generator, further studies were still needed to determine whether the increase in spectra derived from the reactions of •OH with tonalide, PyS^{*} with tonalide, or both. Moreover, it should also be noticed that the subtraction spectra showed a large bleaching from 310 to 380 nm with negative

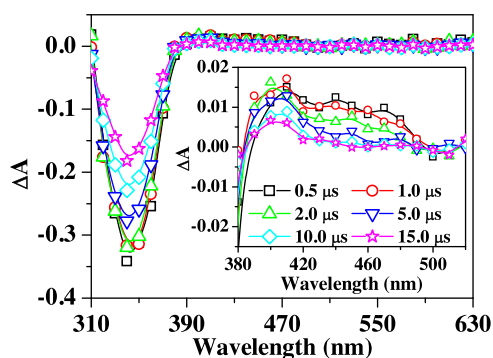


Fig. 3. Spectra obtained by subtracting the spectra of 0.3 mM PSH from PSH-tonalide mixtures (0.3 mM PSH with 0.4 mM tonalide) in acetonitrile under anaerobic conditions with time intervals at 0.5 (□), 1.0 (○), 2.0 (△), 5.0 (▽), 10.0 (◇) and 15.0 μs (☆). Inset of the plot amplified the subtraction spectra ranged from 380 to 520 nm.

peak around 340 nm, which was found similar with the decrease in the transient spectra of pure PSH during photolysis (Fig. 2). Hence, the decrease centered at 340 nm was primarily ascribed to the promoted decomposition of PSH by tonalide, and this suggestion could also be confirmed by the enhanced photo bleaching of PSH (from 310 to 400 nm) observed in mixtures with a higher tonalide concentration (1.25 mM, Supporting Information, Fig. S1). This significant bleaching of PSH from 310 to 380 nm in the PSH-tonalide mixtures could also become an obstacle to observe the intermediates formed from the reaction of $\cdot\text{OH}$ with tonalide. The weak signal of the intermediates originated from $\cdot\text{OH}$ can be covered due to low quality or low absorption coefficients. Considering the coexisting of PyS^{\bullet} and the possible signal covering effects of PSH photo bleaching, the direct characterization of intermediates from the reactions of $\cdot\text{OH}$ with tonalide might not be feasible in these experiments, and more detailed studies were still needed.

To further recognize the intermediates formed specifically from the reaction of $\cdot\text{OH}$ with tonalide, scavenging experiments were performed by adopting 1 M *t*-butanol to quench $\cdot\text{OH}$, and MMA (1 M) to quench both $\cdot\text{OH}$ and PyS^{\bullet} [26]. Then, the intermediates formed from the reaction of $\cdot\text{OH}$ and PyS^{\bullet} with tonalide could be revealed in the subtraction spectra, which was obtained by subtracting the spectra of PSH-tonalide-scavenger mixtures from PSH-tonalide mixtures as shown in Fig. 4a and b, respectively.

The subtraction spectra obtained by *t*-butanol scavenging experiments showed two peaks centered at 360 and 450 nm (Fig. 4a), which were characterized as the intermediates formed from the reactions of tonalide with $\cdot\text{OH}$. The peak at 450 nm decayed fast within 2.0 μs, while the peak at 360 nm was persistent even at 15.0 μs. The unsynchronized decay kinetics indicated these two peaks were not belonged to the same intermediate formed from the reaction of tonalide with $\cdot\text{OH}$. The intermediate at 450 nm could be also observed in Fig. 3, contributed to part of the wide broad increase from 390 to 500 nm. However, the intermediate formed at 360 nm could be then completely covered by the remarkable bleaching of PSH around 355 nm as we concerned above (Fig. 3). To further confirm new intermediate formed in the photo bleaching wavelength at 360 nm by $\cdot\text{OH}$ in PSH-tonalide mixtures, the corresponding time evolution profiles were probed and compared at 340 and 360 nm as shown in the inset of Fig. 2. Since tonalide had no absorbance above 340 nm. Hence, the recovery kinetics at 340 and 360 nm should be all derived from the bleaching of PSH, and the recovery kinetic constants were supposed to be accordant at the both wavelengths. However, in this work, the recovery kinetics was much faster at 360 nm than 340 nm in the PSH-tonalide mixtures, with first order kinetic constant of 3.1×10^5 and $1.5 \times 10^5 \text{ s}^{-1}$, respectively. The significantly higher recovery rate constant at 360 nm indicating the recovery of photo bleaching

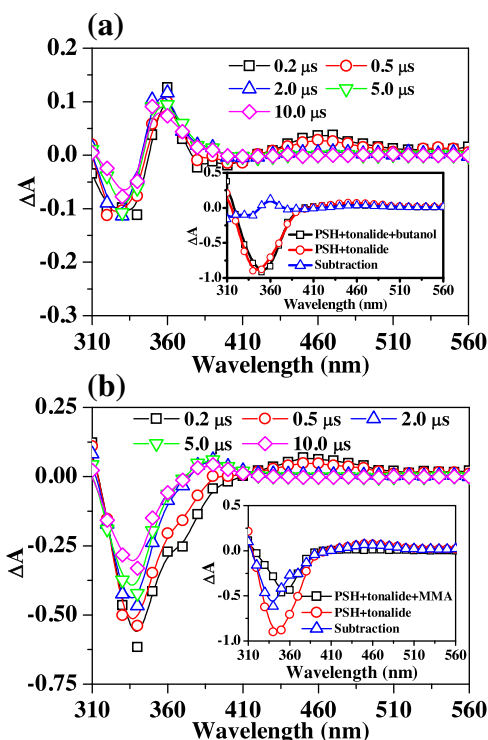


Fig. 4. Subtraction spectra obtained by subtracting the spectra of (a) PSH-tonalide-*t*-butanol and (b) PSH-tonalide-MMA mixtures (0.4 mM PSH, 0.3 mM tonalide and 1 M scavenger) from PSH-tonalide mixtures (0.4 mM PSH and 0.3 mM tonalide) in acetonitrile under anaerobic conditions with time intervals at 0.2 (□), 0.5 (○), 2.0 (△), 5.0 (▽) and 10.0 μs (◇). Insets represent the subtraction spectra (Δ) and the original transient spectra of PSH-tonalide mixtures with (□) and without (○) specific scavenger at 0.2 μs.

PSH was accompanied with the formation of other new intermediate, which further confirmed the formation of new intermediates in the reactions of tonalide with $\cdot\text{OH}$ herein.

To identify and exclude the interferences of intermediates formed from the reactions of PyS^{\bullet} , MMA was further adopted to quench both $\cdot\text{OH}$ and PyS^{\bullet} (Fig. 4b). In accordance with the expectation, the intermediates formed from the reaction of $\cdot\text{OH}$ with tonalide at 360 and 450 nm were also obtained in the subtraction spectra of MMA solutions, characterized by the shoulder peak at 360 nm and the wide peak centered at 450 nm (Fig. 4b). Besides these two intermediates formed by $\cdot\text{OH}$, a new peak was observed at 390 nm which reached its maximum absorption within 2.0 μs. This intermediate may be ascribed to the dimerization product of PyS^{\bullet} [27], and no other significant formation signal was found for the reactions of tonalide with PyS^{\bullet} . Moreover, the bleaching of PSH around 340 nm was significantly inhibited by MMA (Inset of Fig. 4b), indicating MMA might also be a potential quencher for the direct reaction between tonalide and photo-excited PSH.

In sum, no convinced evidence was obtained about the interfacial ROS, PyS^{\bullet} , involved in the reactions with tonalide, and two intermediates were confirmed at 360 and 450 nm during the reactions with $\cdot\text{OH}$. Considering the tonalide was composed of aliphatic structures and a benzene ring, which would both react with $\cdot\text{OH}$ at high bimolecular rate constants [19], these two transient peaks formed by $\cdot\text{OH}$ would be probably assigned to hydrogen abstraction and $\cdot\text{OH}$ addition intermediates of tonalide. Moreover, due to the $\cdot\text{OH}$ addition intermediate would present a more significant red shift phenomenon in the transient absorption spectra as observed in several other reports [31,35], the intermediate formed at 450 nm was further assigned to the $\cdot\text{OH}$ addition intermediate, while the other one at 360 nm was assigned to be formed by

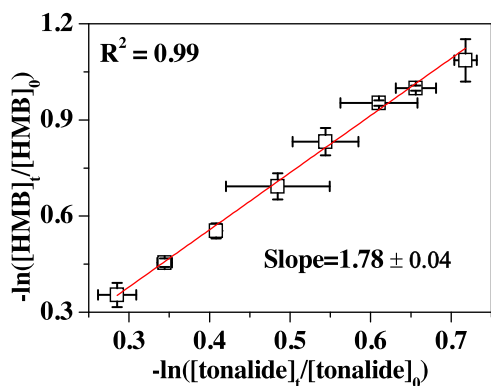


Fig. 5. Competitive $\bullet\text{OH}$ degradation of tonalide and HMB in pure water with $20\ \mu\text{M}$ FeSO_4 and $300\ \mu\text{M}$ H_2O_2 . Value of $k_{\text{tonalide,water}}$ was determined by dividing the slope (1.78) obtained from plot by the value of k_{HMB} .

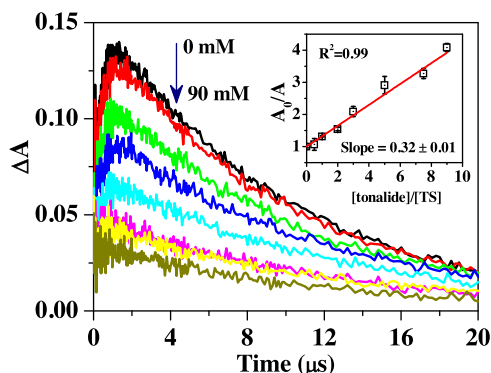


Fig. 6. Kinetics observed for 4 mM TS in anaerobic solutions at 392 nm with 0, 5, 10, 20, 30, 50, 75 and 90 mM tonalide. Inset represents the Stern-Volmer competitive plot as a function of the tonalide/TS relative concentration with a slope of 0.32.

hydrogen abstraction at the methyl substituent or the cyclohexene moiety.

3.3. Bimolecular reaction rate constants for the reaction of tonalide with $\bullet\text{OH}$

Bimolecular rate constant directly reflected the reaction activity of $\bullet\text{OH}$ towards organic compounds. To imitate the decomposition of tonalide in nature environment with and without water, the bimolecular reaction rate constants (k) of tonalide with $\bullet\text{OH}$ were determined both in water and acetonitrile system using Stern-Volmer competitive kinetic analysis, and the value of $k_{\text{tonalide,water}}$ was obtained as $4.04 \times 10^9\ \text{M}^{-1}\ \text{s}^{-1}$ by adopting HMB ($k_{\text{HMB}} = 7.2 \times 10^9\ \text{M}^{-1}\ \text{s}^{-1}$) as the competitive reaction compound as shown in Fig. 5. Similarly, by adopting TS ($k_{\text{TS}} = 6.10 \times 10^9\ \text{M}^{-1}\ \text{s}^{-1}$) as the competitive compound, the rate coefficient for the reaction of $\bullet\text{OH}$ with tonalide in acetonitrile was also measured by determining the dependence of the maximum transient absorbance intensity at 392 nm with the concentrations of tonalide (Fig. 6), and the value of $k_{\text{tonalide,acetonitrile}}$ was obtained as $1.95 \times 10^9\ \text{M}^{-1}\ \text{s}^{-1}$.

Both bimolecular reaction rate constants of $\bullet\text{OH}$ with tonalide obtained in water and acetonitrile solution approach the diffusion-controlled limit, indicated that tonalide could be decomposed fast by $\bullet\text{OH}$ in nature environment, either in water or absorbed in non-aqueous phase. Based on the bimolecular rate constants obtained herein and the level of $\bullet\text{OH}$ in nature aqueous environment (10^{-17} – $10^{-15}\ \text{M}$) [36], the half-life of tonalide degraded by $\bullet\text{OH}$ was estimated to range from 2 to 411 days. Moreover, $k_{\text{tonalide,water}}$ was about 2.1 times as fast as $k_{\text{tonalide,acetonitrile}}$, indicating that

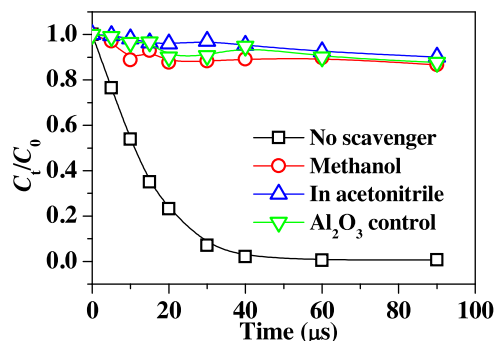


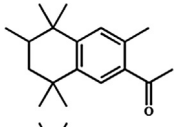
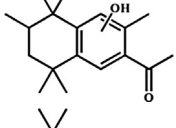
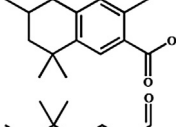
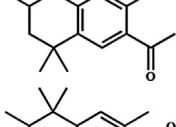
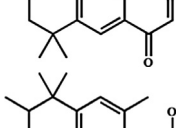
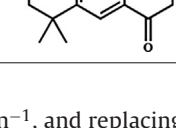
Fig. 7. Photocatalytic degradation kinetics of $50\ \mu\text{M}$ tonalide in $2.0\ \text{g L}^{-1}$ heterogeneous Al_2O_3 or $2.0\ \text{g L}^{-1}$ TiO_2 with no scavenger, 0.1 M methanol, and in pure acetonitrile.

tonalide would be decomposed by $\bullet\text{OH}$ more efficiently in aqueous environment. The increased bimolecular rate constants were also observed for some other organic compounds. For example, the $k_{\text{water}}/k_{\text{acetonitrile}}$ values for benzene and naphthalene were 94.0 and 5.2, respectively [27]. The reason was tentatively suggested that the strong hydrogen bond provided by H_2O could stabilize the transition state of $\bullet\text{OH}$ reaction with organic substrate, finally resulting in higher bimolecular reaction rate constants in aqueous [37]. Considering the strong hydrophobic property of tonalide ($\text{lg}K_{\text{ow}} = 5.7$), as well as other polycyclic musk compounds (obtained higher $\text{lg}K_{\text{ow}}$ values than tonalide, Table S1), the naturally existed of musk residuals in the non-aqueous and nonpolar phases, such as adipose tissue of organisms, and suspended particles mainly composed of organic matter in aqueous, would provide more beneficial conditions for accumulation of polycyclic musk compounds. Because the lowered bimolecular rate constant with $\bullet\text{OH}$ observed herein and the significant accumulation of polycyclic musk in hydrophobic environment, the degradation process and half-life for concentrated tonalide or other polycyclic musk compounds in organic phases are expected to be prolonged in the actual nature aqueous environment. These results implied that when studying the degradation kinetics induced by $\bullet\text{OH}$, the hydrophobicity of specific organic compounds should also be considered carefully due to the variation of the bimolecular reaction rate constant in specific environment.

3.4. Advanced oxidation degradation kinetics, products and toxicity evolution of tonalide

The heterogeneous TiO_2 ($2.0\ \text{g L}^{-1}$) photocatalytic degradation system was selected to study the reaction of $\bullet\text{OH}$ with tonalide because UV- TiO_2 system was an efficient source of $\bullet\text{OH}$ [38]. Firstly, to determine and exclude the directly photolysis effects contributed to the degradation of tonalide, a $2.0\ \text{g L}^{-1}$ Al_2O_3 solution with no photocatalytic effects was used as control (Fig. 7). The pseudo-first-order rate constants (k_1) obtained in TiO_2 heterogeneous system without any scavengers and Al_2O_3 control was obtained as 0.0867 and $0.0017\ \text{min}^{-1}$, respectively (Table S2). These results indicated that the directly photolysis of tonalide was negligible as compared with the photocatalytic degradation, which could be mainly induced by indirect reaction pathways involved several ROSs. Secondly, to further depict the role of $\bullet\text{OH}$ in the degradation of tonalide clearly, methanol was used to scavenge $\bullet\text{OH}$ and h^+ [39], and pure acetonitrile reaction system was further used to characterize the degradation of tonalide in a TiO_2 system with h^+ and totally without $\bullet\text{OH}$ [40,41]. The relative results are shown in Fig. 7 and the k_1 for scavenging degradation kinetic curves were also calculated and are summarized in Table S2. By scavenging with 0.1 M methanol, k_1 decreased from 0.0867 to

Table 1
Products identified by GC-MS of 100 μM tonalide after 30 min photocatalytic degradation.

	Proposed structure	t_R (min)	Molecule weight
A		14.72	258
B		15.73	274
C		15.88	260
D		15.98	272
E		16.74	272
F		17.33	274

0.0022 min^{-1} , and replacing water by acetonitrile decreased k_1 to 0.0013 min^{-1} . These two degradation rate constants were approximately equal to the value obtained in a heterogeneous Al_2O_3 system (0.0017 min^{-1}), where only direct photolysis occurred slightly due to the incompletely light screen effect of optical filter. The scavenging experiments implied that $\bullet\text{OH}$ was almost the only ROS evolved in the photocatalytic degradation of tonalide in a heterogeneous TiO_2 system.

Then, GC-MS was used to probe the main photocatalytic degradation products of tonalide (100 μM) after 30 min. Tonalide and five degradation products were determined with their mass spectra summarized in Fig. S2(a-f), and the possible structures and retention times of the products were proposed as show in Table 1. Generally, the mass spectrum of all five degradation products present the characteristic fragmentation of the parental compound (A), indicate the hydroxylation or oxidation at the cyclohexene moiety of tonalide is rather unlikely occurred in these five degradation products. Based on this proposal, an increase of 16 ($m/z=274$) in the m/z molecular ion of parental compound ($m/z=258$) was then suggested to be the monohydroxylation of tonalide at the aromatic ring (B) and methyl substituent (C). Two compounds identified with $m/z=272$ were suggested to be the ketone derivatives (D and E), which formed by the further oxidation of the hydroxylated products [42]. The $m/z=260$ were tentatively assigned to be the carboxylation of the acetophenone moiety of tonalide (F) as compared with the mass spectra in the literature [43], and the proposed structure of $m/z=260$ could also be found in another oxidation degradation system with sodium hypochlorite as the oxidant [44].

To further probe the potential risk and synergistically toxic effects of tonalide as well as its transformation products attacked by $\bullet\text{OH}$, the evolution of the toxicity of the photocatalytic solution was primarily evaluated using the luminescence of *P. phosphoreum* (Fig. 8). Results showed the relative luminous intensity of *P. phosphoreum* was almost not changed from 0 to 90 min, suggesting

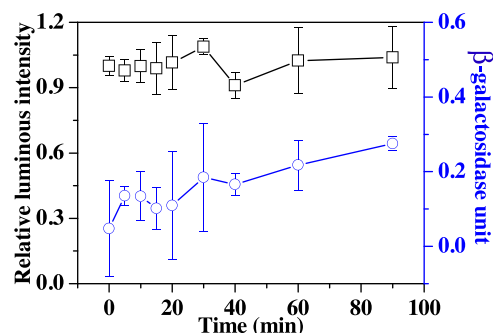


Fig. 8. Evolution of toxicity evaluated with *Photobacterium phosphoreum* (□, left y-axis), and estrogenic activity (○, right y-axis) during 50 μM tonalide solution advanced oxidation with 2.0 g L^{-1} TiO_2 .

the reaction products of tonalide attacked with $\bullet\text{OH}$ were probably not acute toxic. However, considering some products would be further mineralized to CO_2 and H_2O by $\bullet\text{OH}$, the products of $\bullet\text{OH}$ from tonalide could even obtain a little bit higher toxicity than the parental compound. In the aspect of evaluating the toxicity of degradation products to human health, the estrogenic activity evolution of tonalide during the photocatalytic degradation process with $\bullet\text{OH}$ was also investigated. Fig. 8 shows that the estrogenic activity of tonalide solution increased slightly from 0.047 to 0.275 β -galactosidase unit as the reaction progressing from 0 to 90 min, implied the degradation products exhibited relatively higher estrogenic activity than tonalide.

The toxicity analysis of tonalide solution showed similarity trendy with other reports, which have also found the enhanced negative effects of degradation products during the $\bullet\text{OH}$ -initiated reaction of organic compounds [31]. This phenomenon indicated that the traditional environmental and toxicity studies focused only on the concentrations and adverse effects raised by parental compound might not be suitable for the polycyclic musk compounds. Moreover, considering the accumulation of polycyclic musk compounds in hydrophobic environment, and the relatively lower bimolecular reaction rate constant of $\bullet\text{OH}$ with tonalide in non-aqueous phases as confirmed above, the releasing period for the degradation products with adverse effects of this group of compounds would also be prolonged than expected.

4. Conclusions

Based on laser flash photolysis method and subtraction spectra analysis, two transient intermediates with peak at 360 and 450 nm were direct observed from the reactions of tonalide with $\bullet\text{OH}$, providing basic information for further understanding the decomposition mechanisms of polycyclic musk compounds with $\bullet\text{OH}$. The degradation of tonalide with $\bullet\text{OH}$ was fast, while the bimolecular rate constant in acetonitrile were about one half of the reaction constant in aqueous. The variation of rate constants indicated this group of hydrophobic compounds might obtain relatively longer lives when degraded by naturally occurred $\bullet\text{OH}$ than expected, since they were all tend to accumulate in non aqueous phases like sediments or sludge in natural aqueous environment. Moreover, slightly more toxic degradation products were formed during the decomposition process of tonalide, again implying the evaluation on toxicity of organic pollutants should consider both of the parent and transformed degradation products.

Acknowledgments

This work was financially supported by Jiangxi Province Science and Technology Funds for Young Scholars (20151BAB213036) and

National Natural Science Funds for Distinguished Young Scholars (41425015).

Appendix A. Supplementary data

Supplementary data associated with this article can be found, in the online version, at <http://dx.doi.org/10.1016/j.cattod.2016.06.021>.

References

- [1] A. Macherius, T. Eggen, W.G. Lorenz, T. Reemtsma, U. Winkler, M. Moeder, J. Agric. Food Chem. 60 (2012) 7785–7791.
- [2] S. Lignell, P.O. Darnerud, M. Aune, S. Cnattingius, J. Hajslova, L. Setkova, A. Glynn, Environ. Sci. Technol. 42 (2008) 6743–6748.
- [3] A.B. Martinez-Giron, A.L. Crego, M.J. Gonzalez, M.L. Marina, J. Chromatogr. A 1217 (2010) 1157–1165.
- [4] Z.Y. Xie, R. Ebinghaus, C. Temme, O. Heemken, W.G. Ruck, Environ. Sci. Technol. 41 (2007) 5654–5659.
- [5] A.M. Peck, K.C. Hornbuckle, Environ. Sci. Technol. 38 (2004) 367–372.
- [6] H. Song, X.Y. Zeng, Z.Q. Yu, D.L. Zhang, S.X. Cao, W.L. Shao, G.Y. Sheng, J.M. Fu, Environ. Sci. Pollut. R 22 (2015) 1679–1686.
- [7] H. Nakata, H. Sasaki, A. Takemura, M. Yoshioka, S. Tanabe, K. Kannan, Environ. Sci. Technol. 41 (2007) 2216–2222.
- [8] K. Kannan, J.L. Reiner, S.H. Yun, E.E. Perrotta, L. Tao, B. Johnson-Restrepo, B.D. Rodan, Chemosphere 61 (2005) 693–700.
- [9] I.J. Buerge, H.R. Buser, M.D. Muller, T. Poiger, Environ. Sci. Technol. 37 (2003) 5636–5644.
- [10] C.H. Chen, Q.X. Zhou, Y.Y. Bao, Y.N. Li, P. Wang, J. Environ. Sci.–China 22 (2010) 1966–1973.
- [11] G. Carlsson, L. Norrgren, Arch. Environ. Con. Tox. 46 (2004) 102–105.
- [12] M. Breitholtz, L. Wollenberger, L. Dinan, Aquat. Toxicol. 63 (2003) 103–118.
- [13] R. Yamauchi, H. Ishibashi, M. Hirano, T. Mori, J.-W. Kim, K. Arizono, Aquat. Toxicol. 90 (2008) 261–268.
- [14] M. Parolini, S. Magni, I. Traversi, S. Villa, A. Finizio, A. Binelli, J. Hazard. Mater. 285 (2015) 1–10.
- [15] E. Randelli, V. Rossini, I. Corsi, S. Focardi, A.M. Fausto, F. Buonocore, G. Scapigliati, Toxicol. Vitro 25 (2011) 1596–1602.
- [16] T. Luckenbach, D. Epel, Environ. Health Perspect. 113 (2005) 17–24.
- [17] K. Fenner, S. Canonica, L.P. Wackett, M. Elsner, Science 341 (2013) 752–758.
- [18] H. Xu, W.J. Cooper, J. Jung, W. Song, Water Res. 45 (2011) 632–638.
- [19] G.V. Buxton, C.L. Greenstock, W.P. Helman, A.B. Ross, J. Phys. Chem. Ref. Data 17 (1988) 513–886.
- [20] L. Sanchez-Prado, M. Lourido, M. Lores, M. Llompert, C. Garcia-Jares, R. Cela, Rapid Commun. Mass Sp. 18 (2004) 1186–1192.
- [21] J. Santiago-Morales, M.J. Gomez, S. Herrera, A.R. Fernandez-Alba, E. Garcia-Calvo, R. Rosal, Water Res. 46 (2012) 4435–4447.
- [22] P. Calza, V.A. Sakkas, C. Medana, M.A. Islam, E. Raso, K. Panagiotou, T. Albanis, Appl. Catal. B-Environ. 99 (2010) 314–320.
- [23] J. Santiago-Morales, M.J. Gomez, S. Herrera-Lopez, A.R. Fernandez-Alba, E. Garcia-Calvo, R. Rosal, Water Res. 47 (2013) 5546–5556.
- [24] X.W. Liu, Z.L. Chen, L.L. Wang, Y.X. Wu, T. Garoma, J. Photochem. Photobiol. A 230 (2012) 1.
- [25] C. Lange, B. Kuch, J.W. Metzger, J. Hazard. Mater. 282 (2015) 34–40.
- [26] C.H. Chen, R.M. Han, R. Liang, L.M. Fu, P. Wang, X.C. Ai, J.P. Zhang, L.H. Skibsted, J. Phys. Chem. B 115 (2011) 2082–2089.
- [27] M.P. DeMatteo, J.S. Poole, X.F. Shi, R. Sachdeva, P.G. Hatcher, C.M. Hadad, M.S. Platz, J. Am. Chem. Soc. 127 (2005) 7094–7109.
- [28] S. Monadjemi, A. ter Halle, C. Richard, Chemosphere 89 (2012) 269–273.
- [29] S. Monadjemi, M. El Roz, C. Richard, A. Ter Halle, Environ. Sci. Technol. 45 (2011) 9582–9589.
- [30] T.C. An, H.S. Fang, G.Y. Li, S.L. Wang, S.D. Yao, Environ. Toxicol. Chem. 33 (2014) 1809–1816.
- [31] H.S. Fang, Y.P. Gao, G.Y. Li, J.B. An, P.K. Wong, H.Y. Fu, S.D. Yao, X.P. Nie, T.C. An, Environ. Sci. Technol. 47 (2013) 2704–2712.
- [32] H. Yan, H. Wang, J. Chromatogr. A 1295 (2013) 1–15.
- [33] B. Razavi, S. Ben Abdelmelek, W. Song, K.E. O'Shea, W.J. Cooper, Water Res. 45 (2011) 625–631.
- [34] B.M. Aveline, I.E. Kochevar, R.W. Redmond, J. Am. Chem. Soc. 118 (1996) 10113–10123.
- [35] E. Illés, E. Takács, A. Dombi, K. Gajda-Schrantz, G. Rácz, K. Gonter, L. Wojnárovits, Sci. Total Environ. 447 (2013) 286–292.
- [36] X. Zhou, K. Mopper, Mar. Chem. 30 (1990) 71–88.
- [37] S. Mitroka, S. Zimmeck, D. Troya, J.M. Tanko, J. Am. Chem. Soc. 132 (2010) 2907–2913.
- [38] A. Turolla, A. Piazzoli, J. Farner Budarz, M.R. Wiesner, M. Antonelli, Chem. Eng. J. 271 (2015) 260–268.
- [39] A.L. Teel, C.R. Warberg, D.A. Atkinson, R.J. Watts, Water Res. 35 (2001) 977–984.
- [40] Y.X. Chen, S.Y. Yang, K. Wang, L.P. Lou, J. Photochem. Photobiol. A 172 (2005) 47–54.
- [41] A.L. Giraldo, G.A. Peñuela, R.A. Torres-Palma, N.J. Pino, R.A. Palominos, H.D. Mansilla, Water Res. 44 (2010) 5158–5167.
- [42] C. Martin, M. Moeder, X. Daniel, G. Krauss, D. Schlosser, Environ. Sci. Technol. 41 (2007) 5395–5402.
- [43] T.A. Anderson, J.R. Coats, J. Environ. Sci. Heal. B 30 (1995) 473–484.
- [44] P. Andersson, A. Boden, H. Stille, Strait Crossings 2001 (2001) 477–481.